frontiers | Frontiers in Sustainability

ORIGINAL RESEARCH
published: 30 June 2022
doi: 10.3389/frsus.2022.889258

Techno-Economic Optimization of a Low-Temperature Organic Rankine System Driven by Multiple Heat Sources

*Monika Dokl, Zdravko Kravanja and Lidija Čuček**

Laboratory for Process Systems Engineering and Sustainable Development, Faculty of Chemistry and Chemical Engineering, University of Maribor, Maribor, Slovenia

This study presents the optimization of organic Rankine cycle (ORC) which utilizes low temperature waste heat from the aluminum production process and two low temperature renewable energy sources, solar thermal energy and geothermal energy. As geothermal energy is present at lower temperature level compared to the other two heat sources, two separate ORC cycles are considered. Optimization of the proposed system is performed based on a non-linear programming (NLP) formulation by maximizing the thermodynamic and economic performance of the system. The main variables considered in the model include temperature, pressure, flowrate, mass enthalpy, and energy flows of all the streams in the system. To optimize the variables in the system, correlations were developed, which were formulated as NLP models and optimized by minimizing the sum of least squares. The results show that most of the generated power output can be provided by the waste heat, while the lowest by the solar energy due to the relatively low average solar irradiance at considered location. When monthly time periods are considered, the highest electricity production is generated by the working fluid R1245fa in June, and amounts to 830.4 kW from waste heat, 246.5 kW from geothermal energy and 149.4 kW from solar energy. The proposed system is economically feasible for all three studied working fluids and the discount rates of 2% and higher. The final conclusions indicate that the proposed ORC system utilizing waste heat, geothermal and solar thermal energy, can generate power in a more sustainable way.

Keywords: organic Rankine cycle, low-temperature energy sources, multiple energy sources, industrial waste heat, solar thermal, geothermal energy, techno-economic optimization

OPEN ACCESS

Edited by:
Adeniyi Jide Isafiade, University of Cape Town, South Africa

Reviewed by:
Santanu Bandyopadhyay, Indian Institute of Technology Bombay, India
Mauro Antonio Da Silva Sá Ravagnani, State University of Maringá, Brazil
David Esteban Bernal Neira, National Aeronautics and Space Administration, United States

***Correspondence:**
Lidija Čuček
lidija.cucek@um.si

Specialty section:
This article was submitted to Sustainable Chemical Process Design, a section of the journal Frontiers in Sustainability

Received: *04 March 2022*
Accepted: *08 June 2022*
Published: *30 June 2022*

Citation:
Dokl M, Kravanja Z and Čuček L (2022) Techno-Economic Optimization of a Low-Temperature Organic Rankine System Driven by Multiple Heat Sources. Front. Sustain. 3:889258. doi: 10.3389/frsus.2022.889258

INTRODUCTION

The growth of global energy demand, the associated negative environmental impacts and the limited availability of fossil fuel resources led to the developments in renewable energy systems. Renewable energy sources have been widely used to produce heat and electricity; however, their main limitation lies in their variability due to changes in meteorological conditions. Hybrid energy systems have been proposed to overcome the limitations of a single renewable energy source and thus increasing reliability of energy generation (Zhang et al., 2020).

Besides renewable energy, energy recovery from industrial processes could represent a considerable source of energy. Over 50% of the total energy used in the world is discharged as a

waste heat (Mahmoudi et al., 2018). It was estimated that about 20% of the US electricity could be produced by waste heat recovery from US industrial facilities (Castelli et al., 2019). Similarly, in Europe, industrial waste heat sources could cover at least 25% of potential district heat production (Angelino et al., 2021). However, the low temperature waste heat make difficulties for its recovery within the process (Anastasovski et al., 2020). Besides, there are various barriers for waste heat utilization, such as low quality heat, unstable source of heat, lack of heat demand, high investment cost and other (Wahlroos et al., 2018).

Renewable energy sources and utilization processes could be classified according to temperature in three levels: low temperature, medium temperature, and high temperature. Low temperature heat is below 150°C, medium temperature heat between 150 and 400°C and high temperature heat above 400°C (Epp and Oropeza, 2017). However, different authors have used different temperature ranges for each level (Angelino et al., 2021). Among low temperature renewable energy sources are geothermal and solar thermal and also waste heat from industrial and other sources (Angelino et al., 2021). Geothermal heat source varies in temperature from 50 to 350°C, of which geothermal water temperature is mostly below 220°C (Sun et al., 2020). Small-scale solar systems, such as flat plate collectors produce thermal energy with temperature of <100°C (Angelino et al., 2021). Waste heat includes heat streams in the form of exhaust gases or effluents at various temperature levels (Christodoulides et al., 2022). Significant amounts of waste heat potential corresponds to a low temperature waste heat (Papapetrou et al., 2018).

In recent years, many investigations have been conducted on the combination of different renewable energy sources and waste heat with power production systems, such as organic Rankine cycle (ORC) and Kalina cycle (Jahangir et al., 2019). ORC is the usual choice and is mature technology for low temperature heat energy conversion to electricity to improve energy efficiency (Zhang et al., 2018). It has been extensively investigated and commercially implemented in various industrial and domestic applications (Lecompte et al., 2017). Until recently existing studies have never combined the use of more than one heat source in a single cycle (Gomaa et al., 2020). The use of ORC integrated with multiple heat sources has been investigated for electricity generation from geothermal energy as the primary heat source and waste heat from biogas engine as the secondary heat source (Toselli et al., 2019). In addition, a ORC system combined with solar energy and waste heat (Bellos and Tzivanidis, 2018), a Rankine cycle powered by biomass and solar energy (Anvari et al., 2019) and a geothermal-solar ORC (Senturk Acar and Arslan, 2019) have been studied. Recent studies related to ORC have mainly focused on the utilization of low-grade heat sources, selection of the most appropriate working fluids and mixtures, experimental studies (Pang et al., 2017), and design of ORC system (Chen et al., 2010).

Abbreviations: GAMS, General Algebraic Modelling System; GWP, Global Warming Potential; NLP, Nonlinear Programming; NPV, Net Present Value; NRTL, Non-Random Two-Liquid; ODP, Ozone Depletion Potential; ORC, Organic Rankine Cycle; REFPROP, REFerence fluid PROPerties.

However, literature review has shown that existing studies are usually focused on only one energy source for an ORC system, either waste heat or renewable energy sources (Gomaa et al., 2020), such as solar, geothermal, biomass and heat from heat pumps. A review of ORC systems using geothermal energy revealed that the choice of working fluid and the configuration and architecture of the cycle have an important impact on system performance (Haghighi et al., 2021). A literature review on ORC system driven by solar thermal collectors reported high efficiencies (up to 20%) when concentrating solar collectors are applied, while the performance of non-concentrating technologies turned out to be better in cooler and more overcast climates, leading to the overall conclusion that solar ORC is a suitable option for renewable power generation (Loni et al., 2021a). A recent review on waste heat recovery from aluminum industry revealed that limited studies have been made to recover heat using Rankine cycles (Brough and Jouhara, 2020). Further it was pointed out that the challenge regarding ORC is improvement of its thermodynamic performance and the competitiveness (Loni et al., 2021b). In order to maximize system efficiency and to reduce the investment cost, the optimization of the system should be performed to improve ORC design.

In this study, the thermodynamic and economic performances of an ORC system integrating a combination of three low-temperature heat sources, industrial waste heat, solar thermal and geothermal energy are investigated. Optimization of the combined ORC system is performed maximizing the power output of the turbines and the revenue from electricity and heat production. The data regarding waste heat and meteorological data were obtained from an aluminum company, the data regarding geothermal energy from a local report (LEA Ptuj, 2010), and the data regarding fluid properties were obtained from Aspen Plus (Aspen Technology, 2022). Due to similar temperature levels (≈85°C at the inlet to evaporator), both industrial waste heat and solar energy are utilized in one cycle, while geothermal energy (55°C at the inlet to evaporator) uses separate cycle due to lower temperature level.

This study is based on an optimization approach developed in previous research of heat pump enhanced solar thermal (Abikoye et al., 2020) and optimizing ORC for waste heat recovery (Dokl et al., 2021). The operating features in the ORC are defined as variables to be optimized, while correlations were developed for the thermodynamic properties of fluids. ORC is formulated with a flowsheet structure and all the components in the system are modeled with corresponding equations. In the circuit, three working fluids are studied and compared. Compared to the previous work (Dokl et al., 2021), this study further develops optimization of ORC for solar and geothermal integration, where significant extensions were required to integrate the two selected renewable sources.

METHODOLOGY

In this study, the multiple heat source utilization system based on Rankine technology is investigated in terms of thermodynamic and economic performance. In this section, first the proposed design of ORC system is explained and further the description of the mathematical formulation is presented.

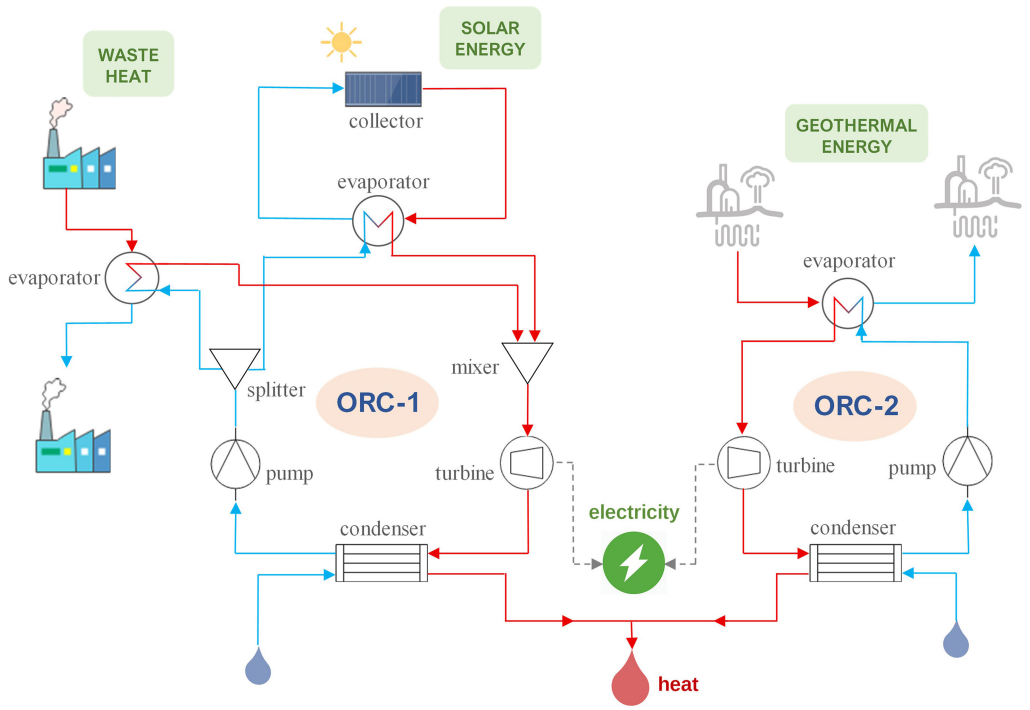

FIGURE 1 | Schematic representation of proposed system.

Description of ORC System

In this section, multiple low-temperature heat source utilization system is described. ORC power generation system consists of two ORC loops, each of which consists of three subsystems: the heat source system, the ORC system, and the cooling system or heat sink. **Figure 1** shows the schematic diagram of two cycles that jointly generate electricity and hot water. Due to the similar temperature range, industrial waste heat and solar thermal are used as combined sources in one cycle, while geothermal uses a separate cycle due to its lower temperature range. As for the possible configurations of the ORC unit, a basic design is considered for both cycles. Regardless of a rigid design in terms of the number of streams and process units, their sizing is subject to the optimization and the variables of the system are optimized to obtain the best performance.

The basic principle of ORC is the circulation of organic working fluid with a low-boiling point that absorbs thermal energy from the heat source to produce electricity. The process consists of four units, two heat exchangers (evaporator and condenser) and two pressure changers (turbine and pump). In the evaporator, the working fluid is evaporated by receiving thermal energy from the heat source and then sent to the turbine where during the expansion process electricity is produced. The low-pressure vaporized fluid enters the condenser, where the cooling source and the condensing working fluid exchange heat. The fluid then passes through the pump and completes the circuit at the inlet of the evaporator as high-pressure liquid.

The properties of the working fluid for heat transfer have a significant impact on the performance of the system. The selection criteria regarding thermodynamic properties of a working fluid must consider the critical temperature of the working fluid, which should not be lower than the highest temperature in the circuit to maintain the operating conditions of the system in the subcritical range, and the condensing pressure should be higher than the atmospheric pressure to avoid suction of the outside air. In addition, the working fluid should be thermally stable and have low viscosity and high heat transfer coefficient to improve performance of the system. In terms of system economics, working fluids with low price and easy access are beneficial. To curb environmental concerns and to meet safety requirements, toxic, and flammable fluids and the fluids with high Ozone Depletion Potential (ODP) and Global Warming Potential (GWP) should be avoided in the selection process.

In this study, the thermodynamic and economic performance of the system is investigated considering the three organic working fluids selected. The following working fluids are studied and compared, R245fa, R1234yf, and R1234ze, which were found to be appropriate fluids for low-temperature waste heat recovery (Yang et al., 2021) and are suitable fluids according to the criteria mentioned above. Some physical properties of the studied working fluids (e.g., boiling and critical temperature, specific heat of liquid and vapor, GWP and ODP) are collected in published article (Dokl et al., 2021).

For solar thermal exploitation, ORC is connected to the solar collectors by a closed loop with circulating heat transfer fluid assumed as the ethylene glycol-water mixture. The input data regarding solar energy use such as solar irradiance and ambient temperature are collected by aluminum industry as collectors are positioned near the company. Additionally, as a

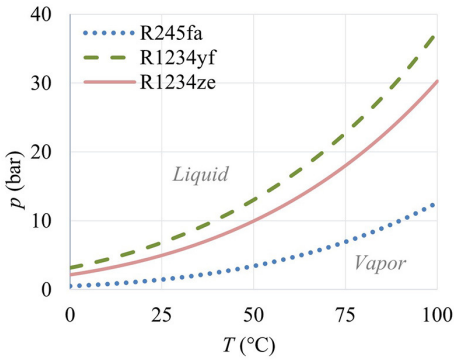

FIGURE 2 | Liquid vapor pressure for used working fluids.

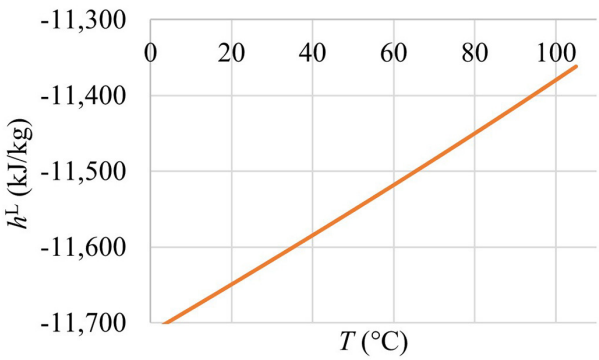

FIGURE 3 | Liquid mass enthalpy of ethylene glycol-water mixture.

waste heat source, flue gas from aluminum smelter is applied, considering the data of flue gas temperature, flowrate, pressure and composition as input conditions provided by aluminum company (Dokl et al., 2021). The data concerning geothermal heat located near the aluminum industry was based on the local resource assessment report (LEA Ptuj, 2010), while the data regarding thermodynamic properties of fluids used in the system is obtained from Aspen Plus (Aspen Technology, 2022).

Description of Mathematical Model

To optimize the operating conditions according to defined objectives mathematical model of the proposed design is developed. The work follows the basic concept of the ORC presented in the previous work by authors (Dokl et al., 2021), while the current study provides the optimization framework with several extensions and additions described in the following.

In the literature usually the one period nature of optimization models is considered when studying such systems (Dokl et al., 2021). To achieve lower level of model complexity and reduce computation time, the model is structured in a single period manner, addressing the 1-year average input data.

Development of Correlations for Obtaining the Relations of Variables

To optimize the operating conditions of the system, correlations as functions of temperature or pressure or both were developed.

TABLE 1 | Values of optimized coefficients for obtaining correlations for specific enthalpy of ethylene glycol-water mixture.

C1	$-1.26{\cdot}10^{5}$
C2	$2.98{\cdot}10^{-1}$
C3	$-9.75{\cdot}10^{5}$
C4	$5.71{\cdot}10^{-3}$
C5	$1.27{\cdot}10^{6}$
C6	$7.20{\cdot}10^{-2}$
C7	$-1.32{\cdot}10^{2}$
C8	$-1.49{\cdot}10^{6}$
C9	$1.28{\cdot}10^{-1}$
C10	$-8.83{\cdot}10^{5}$
C11	$1.75{\cdot}10^{-2}$
C12	$5.30{\cdot}10^{-1}$
C13	$3.35{\cdot}10^{-1}$

Variables such as vapor (h^{V}) and liquid (h^{L}) mass enthalpy, liquid vapor pressure (p^{L}), heat capacity ratio (c_p/c_V), irreversibility in the turbine (η_{irrev}), temperature difference in the pump (T^{in}/T^{out}) were modeled by different types of equation, including linear and exponential terms. The equations for h^{V}, h^{L}, p^{L}, c_p/c_V, η_{irrev}, T^{in}/T^{out} for working fluids, h^{V} for flue gas, and h^{L} for cooling water dependence on temperature and/or pressure are comprehensively described in previous work (Dokl et al., 2021). An example of the liquid vapor pressure (p^{L}) for the three different studied working fluids is shown in **Figure 2**, which is modified from Dokl et al. (2021).

Besides the fluids such as working fluids, flue gas and water, mixture of 50% ethylene glycol and 50% water is assumed for the solar closed circuit due to possible lower ambient temperatures in the circuit during colder seasons. The operating conditions of this loop are determined depending on the liquid specific enthalpy with temperature, as shown in **Figure 3**, while the pressure in this loop is assumed to be constant (1 bar).

To optimize the flowrate and temperature of the ethylene glycol-water mixture, the correlation for the liquid mass enthalpy is developed as a function of temperature, as shown in Equation (1). The sum of squared errors between calculated and given data was obtained in 9.83 s and was acceptably small ($1.04{\cdot}10^{-2}$). The number of given values to achieve the best fit was 1,041. The optimized values of the coefficients (C1–C13) were obtained using CONOPT solver in GAMS on a personal computer with an Intel® Core™ i7-10750H CPU @ 2.60 GHz processor with 16 GB of RAM and are summarized in **Table 1** rounded to two decimal points for clarity.

$$h^{L}_{EGW} = C1 + C2 \cdot T^{C3} + C4 \cdot T^{C5} + C6 \cdot T^{C7} + C8 \cdot T^{C9} + C10 \cdot \exp(T^{C11}) + C12 \cdot \exp(T^{C13}) \quad (1)$$

Mathematical Model for ORC System

Schematic representation of the proposed system shown in **Figure 1** is used as a basis for the development of ORC design. The detailed description of mathematical model including the assumptions is given in the previous paper by the authors (Dokl et al., 2021). Compared to the previous work, the mathematical model for solar thermal integration is additionally included and economic objective is modified to consider maximization of the

revenue obtained from selling the heat and power produced from the system.

$$T(p, q_{\mathrm{m}}, h)_{\mathrm{u,out}} = T(p, q_{\mathrm{m}}, h)_{\mathrm{u1,in}} \quad \forall (in, out) \in IO, (u, u1) \in \{evap, turb, cond, pump, mix, split, coll\} \tag{2}$$

The model is formulated as a flowsheet structure as in reference (Dokl et al., 2021), where the connections between process units are:

The streams between the units are characterized with variable temperature (T), pressure (p), flowrate (q_{m}) and specific enthalpy (h), which are the same at the outlet (out) of process unit u and the inlet (in) of next process unit $u1$. The following process units are considered in the ORC and solar collector loops: three evaporators (*evap*), one for each heat source, two turbines (*turb*), two condensers (*cond*) and two pumps (*pump*), one in each ORC loop, one mixer (*mix*), and splitter (*split*) for mixing and splitting of fluid before the turbine and after the pump and solar collector (*coll*) which absorbs solar radiation and converts it to thermal energy.

In evaporators and condensers, the heat is passed from heat source to working fluid or from working fluid to heat sink, where heat duty in heat exchanger (Q_{u}) is calculated as shown in Equation (3) with operator $\pm$ showing the direction of energy flow:

$$Q_{\mathrm{u}} = \pm q_{\mathrm{m,u}} \cdot (h_{\mathrm{u,out}} - h_{\mathrm{u,in}}), \forall u \in \{evap, cond, coll\} \tag{3}$$

The electricity is generated in the turbine and calculated by Equation (4), where parameter η_{turb} indicates the mechanical efficiency, which assumes that 85% of energy contained in working fluid is converted into power.

$$W_{\mathrm{turb}} = q_{\mathrm{m,turb}} \cdot (h_{\mathrm{turb,out}} - h_{\mathrm{turb,in}}) \cdot \eta_{\mathrm{turb}} \tag{4}$$

For all the details related to the calculation of variables in the ORC system, the reader is referred to the previous work by the authors (Dokl et al., 2021). In this reference (Dokl et al., 2021), description of equations is provided for material balances [see Equation (2)], pressure level through evaporator and condenser [see Equation (3)], thermal energy flow in evaporator [see Equation (4)] and condenser [see Equation (5)], minimum approach temperature constraints in evaporator [see Equations (6, 7)] and condenser [see Equations (8, 9)], liquid-vapor phase change relations [see Equation (10)–(12)], irreversibility in the turbine and heat capacity ratio [see Equation (13)].

Mathematical Model for Solar Thermal Integration

Solar thermal energy is supplied to the system by solar collectors. An evacuated tube solar collector is considered for the design (Abikoye et al., 2019), which can achieve similar temperature levels during its operation and waste heat from aluminum smelter. The heat gained by the collector (Q_{coll}) is a function of collector area (A_{coll}), irradiance on the collector (E), the difference in average temperature of the fluid passing the collector ($T_{\mathrm{coll,in}} + T_{\mathrm{coll,out}})/2$) and ambient temperature (T_{amb}), as shown in Equation (5):

$$Q_{\mathrm{coll}} = A_{\mathrm{coll}} \cdot \left(\Pi_0 \cdot E - a_1 \cdot \left(\frac{T_{\mathrm{coll,in}} + T_{\mathrm{coll,out}}}{2} - T_{\mathrm{amb}} \right) - a_2 \cdot \left(\frac{T_{\mathrm{coll,in}} + T_{\mathrm{coll,out}}}{2} - T_{\mathrm{amb}} \right)^2 \right) \tag{5}$$

where Π_0 is solar efficiency factor and a_1 and a_2 are experimental constants, adopted from the literature (Isafiade et al., 2016). The balance for heat captured by the fluid is as shown in Equation (6):

$$Q_{\mathrm{coll}} = q_{\mathrm{m,coll}} \cdot (h_{\mathrm{coll,out}} - h_{\mathrm{coll,in}}) \tag{6}$$

The data regarding solar irradiance and ambient temperature are given annually on an hourly basis. To investigate the multiple heat source utilization by proposed heat recovery technology the input data is simplified to consider the average values and thus the model is formulated as a single-period model assuming steady state conditions. The data are averaged based on the model reduction techniques (Lam et al., 2011), clustered into hourly, daily and monthly periods similar to the previous work by authors (Egieya et al., 2020). Clustering of solar irradiation data is shown in Equation (7) and the data for ambient temperature in Equation (8), where E and T_{amb} are average solar irradiation and ambient temperature. In Equations (7) and (8), E and T_{amb} are hourly solar irradiation and ambient temperature data for each hour of the year. The sets *MPOM*, *DPOD*, and *HPOD* designate set of pairs of maximal number of time periods in a year (*mpo*, *dpo*, and *hpo*) and merged time periods (*mp*, *dp*, and *hp*).

By employing such a model reduction method, the 24 h of a day can be discretized into any number of merged hours, the 28–31 days of a month into the same or smaller number of merged days, and the 12 months of a year into the 12 or smaller number of merged months. However, to simplify the problem by reducing the problem size and shortening the computational time, one merged period accounting for the data of 1 year is assumed. Further, to account for variations in solar irradiance and ambient temperature, sensitivity analysis is performed considering the multi-period model and average meteorological data for each of the 12 monthly time periods.

$$E_{\mathrm{mp,dp,hp}} = \frac{\sum_{mpo \in MP} \sum_{dpo \in DP} \sum_{hpo \in HP} \bigwedge_{(mpo,mp) \in MPOM, (dpo,dp) \in DPOD, (hpo,hp) \in HPOH, (dpo,mpo) \in DPM} E'_{\mathrm{mp,dp,hp}}}{\left(\sum_{mpo \in MP} \bigwedge_{(mpo,mp) \in MPOM} |mpo| \cdot \sum_{dpo \in DP} \bigwedge_{(dpo,dp) \in DPOD} |dpo| \cdot \sum_{hpo \in HP} \bigwedge_{(hpo,hp) \in HPOH} |hpo| \right)}, \quad \forall mp \subseteq MP, dp \subseteq DP, hp \subseteq HP, (dp, mp) \subseteq DPM \tag{7}$$

$$T_{\text{amb,mp,dp,hp}} = \frac{\sum_{mpo\in MP}\sum_{dpo\in DP}\sum_{hpo\in HP}\bigwedge_{(mpo,mp)\in MPOM,(dpo,dp)\in DPOD,(hpo,hp)\in HPOH,(dpo,mpo)\in DPM} T'_{\text{amb,mp,dp,hp}}}{\left(\sum_{mpo\in MP}\bigwedge_{(mpo,mp)\in MPOM}|mpo|\cdot\sum_{dpo\in DP}\bigwedge_{(dpo,dp)\in DPOD}|dpo|\cdot\sum_{hpo\in HP}\bigwedge_{(hpo,hp)\in HPOH}|hpo|\right)},$$
$$\forall mp\subseteq MP, dp\subseteq DP, hp\subseteq HP, (dp,mp)\subseteq DPM \quad (8)$$

Economic Analysis

The economic performance of the system is examined in terms of capital investment and annual cash flows (revenue and operating cost). The capital cost investment (C_{TCI}) is calculated as the sum of purchase cost of process equipment and other cost associated with installation and piping, instruments and controllers, lighting and electrical materials, spare materials, insulation, construction overhead, contractor engineering expenses, site preparation or development, utilities and industrial buildings, offsite facilities and contingencies. The cost of process units in the plant is calculated using the factored-cost method (Seider et al., 2009), applied to a current year using cost indexes, while the cost of the solar collector is for simplicity assumed as in the literature (Isafiade et al., 2016). Referring to the studies that include economic analysis of ORC system, such as optimization of ORC for waste heat recovery from gas turbine (Pierobon et al., 2013) and Diesel engine (Kalikatzarakis and Frangopoulos, 2015) and optimization of ORC for geothermal energy exploitation (Walraven et al., 2015) by considering zeotropic mixtures and pure fluids as working fluids (Andreasen et al., 2021), single life for all components of ORC is assumed for simplicity.

The estimation of operating cost (C_{OC}) consists of maintenance, depreciation, labor, utilities, and other cost. In addition, economic parameters such as net present value (NPV) and payback period (t_{PB}) are calculated based on the discounted cash flow method as presented in previous work (Dokl et al., 2021). For the calculation, the following values of economic parameters are assumed, the electricity price (c_{elec}) is 0.08 €/kWh, the heat price (c_{heat}) is 0.0243 €/kWh (the value considers also investment in district heating), the discount rate (p) is 8%, the lifetime of the system (N) is 20 y, and the number of annual operating hours (t_{OH}) is 8,760 h/y. Due to the strong influence of the discount rate on the economic performance of the system (Walraven et al., 2015; Zore et al., 2018), sensitivity analysis is performed in this regard, changing the p from 2 to 14%.

Objectives of the Study

Thermodynamic and economic performance of the ORC system are studied by optimization with two objectives, maximization of power output, and the revenue from selling the heat and electricity. The optimized operating conditions of the ORC energy system that maximizes power output of the turbines (W_{sys}) are determined for each working fluid as follows:

$$\max W_{\text{sys}} = \max(q_{\text{m,turb-1}}\cdot(h_{\text{turb-1,out}} - h_{\text{turb-1,in}})\cdot\eta_{\text{turb-1}} + q_{\text{m,turb-2}}\cdot(h_{\text{turb-2,out}} - h_{\text{turb-2,in}})\cdot\eta_{\text{turb-2}}) \quad (9)$$

where subscripts 1 and 2 refer to the ORC cycles in the system (ORC-1 and ORC-2), see also **Figure 1**.

The second objective studied is the maximization of the revenue of the system (R_{sys}) obtained from selling the power produced in the turbines and the heat contained in the water at the outlet of the condensers for each working fluid. Depending on the amount of electricity obtained by the two turbines ($W_{\text{turb-1}}$ and $W_{\text{turb-2}}$), price of electricity (c_{elec}), heat duty of the two condensers ($Q_{\text{cond-1}}$ and $Q_{\text{cond-2}}$), price of heat (c_{heat}), and number of operating hours per year (t_{OH}), the joint revenue from production of electricity and heat is obtained as shown in Equation (10). The general calculation of revenue is adopted from the previous work (Dokl et al., 2021).

$$\max R_{\text{sys}} = \max((c_{\text{elec}}\cdot(W_{\text{turb-1}} + W_{\text{turb-2}}) + c_{\text{heat}}\cdot(Q_{\text{cond-1}} + Q_{\text{cond-2}}))\cdot t_{\text{OH}}) \quad (10)$$

CASE STUDY

The optimization of the ORC system is carried out on the case study of a municipality of Kidričevo which is located in northeastern in Slovenia. In this municipality, the company is based specialized in producing aluminum products. Optimization of ORC system utilizing waste heat and solar thermal energy is performed on the case study of aluminum company, while low-temperature geothermal energy is also available in the vicinity of the aluminum industry.

Aluminum production is one of the most energy-intensive processes, where about half of the consumed energy is lost as waste heat. In this study, exploitation of thermal energy contained in the flue gas from aluminum smelter, which accounts for around 40% of the waste heat, is considered. The flue gas is composed of 77.34% nitrogen, 20.82% oxygen, 1.73% CO_2, 0.09% CO and small amounts of HF ($1.6\cdot10^{-5}$%), SO_2 ($7.7\cdot10^{-3}$%), CF_4 ($2.1\cdot10^{-5}$%), and C_2F_6 ($2.0\cdot10^{-6}$%) (Dokl et al., 2021). Along with flue gas composition, flue gas data for temperature, pressure and flowrate are provided on an hourly basis by the aluminum company. For simplification, the annual average values based on the data obtained from the company for 2019 were considered and serve as input parameters for the ORC system. The outlet temperature of flue gas is 84.2°C, pressure is 1 bar, and flow rate is 204.5 kg/s.

The solar energy input data consists of hourly solar radiation and ambient temperature data collected and provided by the aluminum company along with the waste heat data. Examples of monthly and daily hourly solar irradiance data in a typical winter and summer month are illustrated on **Figures 4**, **5**. The red line in Figures shows the average of the data presented. For simplification, the annual average values of solar irradiation and ambient temperature data are considered and are calculated to be 153.5 W/m^2 and 11.8°C. Another important parameter related

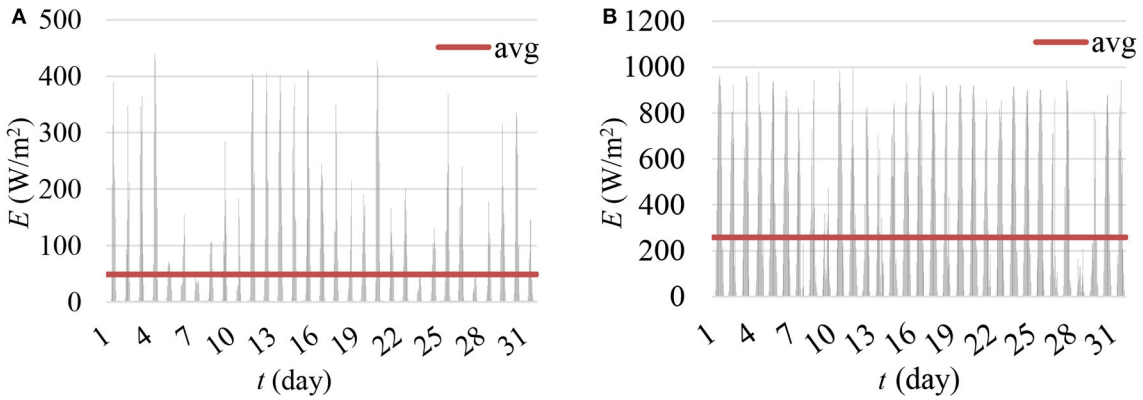

FIGURE 4 | Hourly and average solar irradiation data for **(A)** winter month (January 2019) and **(B)** summer month (July 2019).

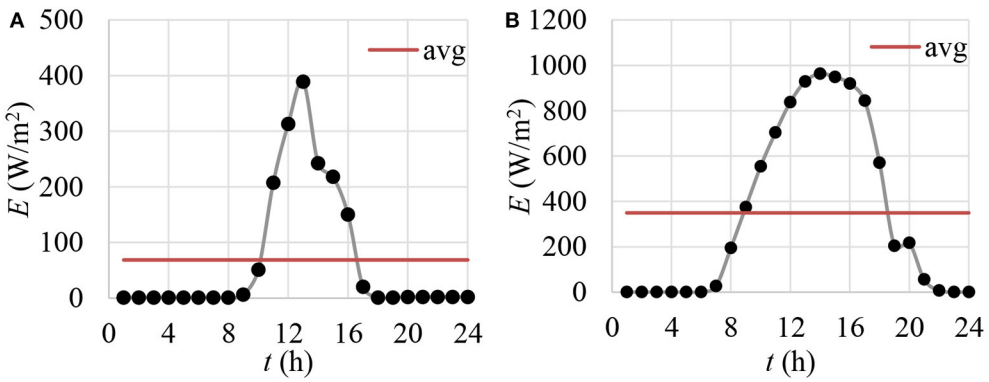

FIGURE 5 | Hourly and average irradiation for **(A)** typical day in winter (1st January 2019) and **(B)** typical day in summer (1st July 2019).

to the utilization of solar thermal is the area of solar collectors, which is assumed to be constant throughout the year and covers an area of 10,000 m^2.

Among low-temperature renewable energy sources, geothermal energy is available in the spatial area considered. The numerous low-temperature hot water springs have the exploitation potential of flowrate of around 100 L/s and temperature range of 40–70°C, where in the case study the average water temperature of 55°C is assumed. The geothermal heat source data is based on the local resource assessment report (LEA Ptuj, 2010).

Similar to the previous study (Dokl et al., 2021), the values of other input parameters such as cooling water temperature and pressure (T_{water} is 25°C and p_{water} is 1 bar) and minimum approach temperature in heat exchangers (ΔT_{min} is 5°C) are considered. The value of ΔT_{min} has a great impact on the size of heat exchangers and consequently on the performance of the system, since a compromise is achieved between the heat exchanger cost and the power output of the system. Lower ΔT_{min} values allow for better utilization of the thermal energy of the heat source while at the same time represent an economic disadvantage in the form of high capital cost for heat exchangers.

The data for various thermodynamic properties such as liquid and vapor specific enthalpy, heat capacity ratio and liquid vapor pressure of used fluids (namely: R245fa, R1234yf, R1234ze, water, flue gas, ethylene glycol/water mixture) are collected from Aspen Plus (Aspen Technology, 2022), where for flue gas and ethylene glycol-water mixture thermodynamic method NRTL is considered and for other fluids thermodynamic method REFPROP is used.

Referring to the average input parameters related to the heat sources, the model is structured in a single period manner, addressing the 1-year average input data as noted above. The design for integration of multiple low-temperature heat sources is modeled and solved in GAMS. The formulated single-period NLP model consists of 245 single equations and 257 or 260 single variables (first or second objective), while multi-period model consists of 2,925 single equations and 2,738 or 3,087 single variables (first or second objective). The solutions to the model are provided in less than a second for single-period and <3 s for multi-period model using CONOPT solver in GAMS with 0.1% optimality gap. The solutions are obtained on a personal computer with an Intel® Core™ i7-10750H CPU @ 2.60 GHz processor with 16 GB of RAM.

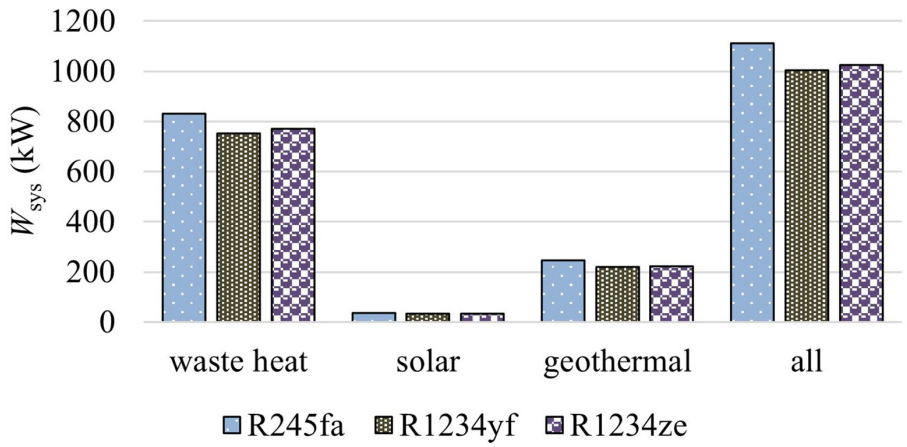

FIGURE 6 | Maximum values of power output regarding heat sources and working fluids for optimized ORC system.

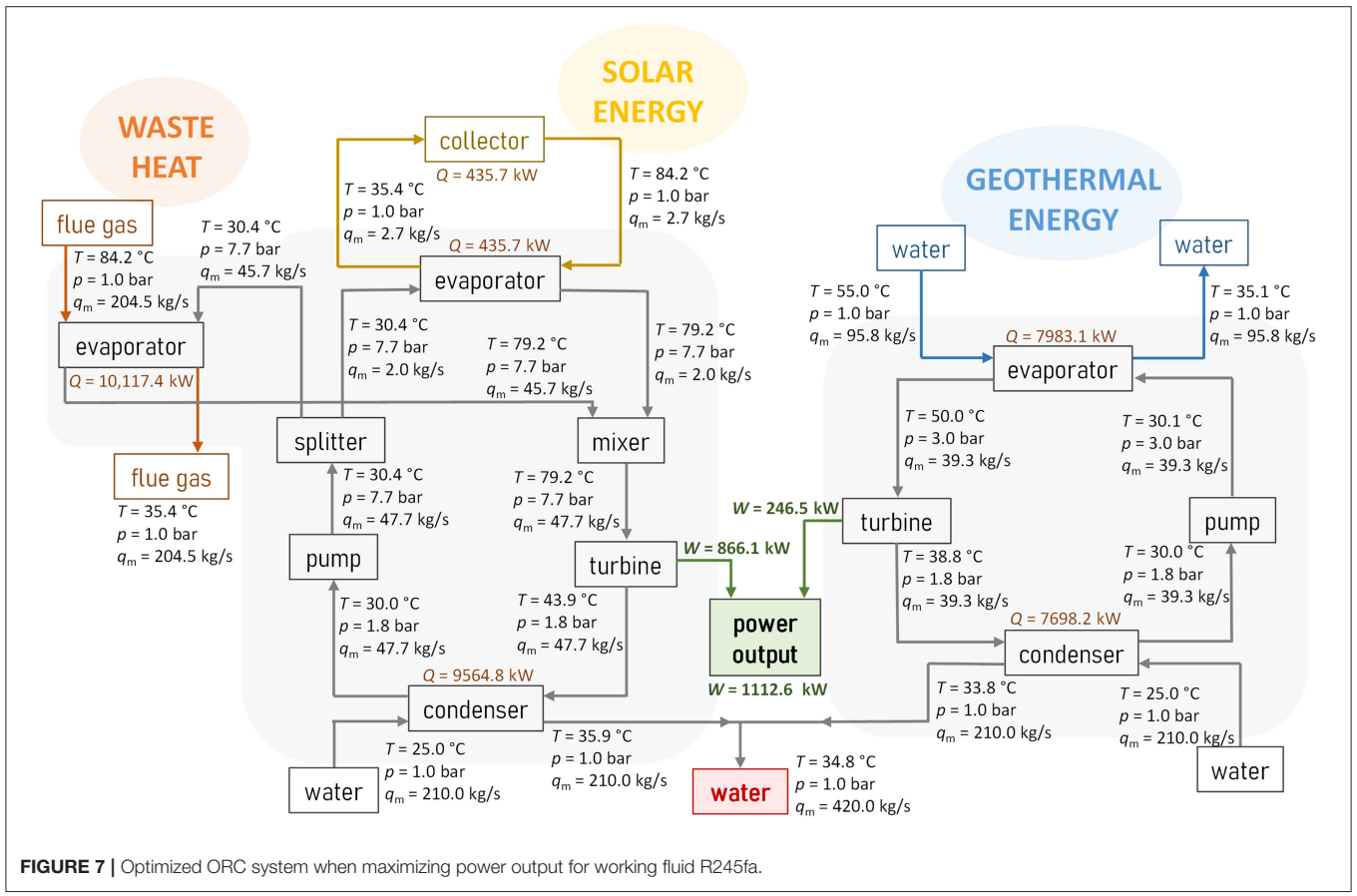

FIGURE 7 | Optimized ORC system when maximizing power output for working fluid R245fa.

RESULTS AND DISCUSSION

In this study, the optimization process of the cogeneration system based on ORC technology is performed for three different working fluids (R245fa, R1234yf, R1234ze). First, the thermodynamic performance of the system is optimized by maximization of power output and further economic optimization is performed with respect to the highest revenue generated from electricity and heat production.

Maximizing Power Output

The operating conditions of the system are optimized to achieve the maximum electricity production from the turbines. **Figure 6** shows maximum values of power output separately for each

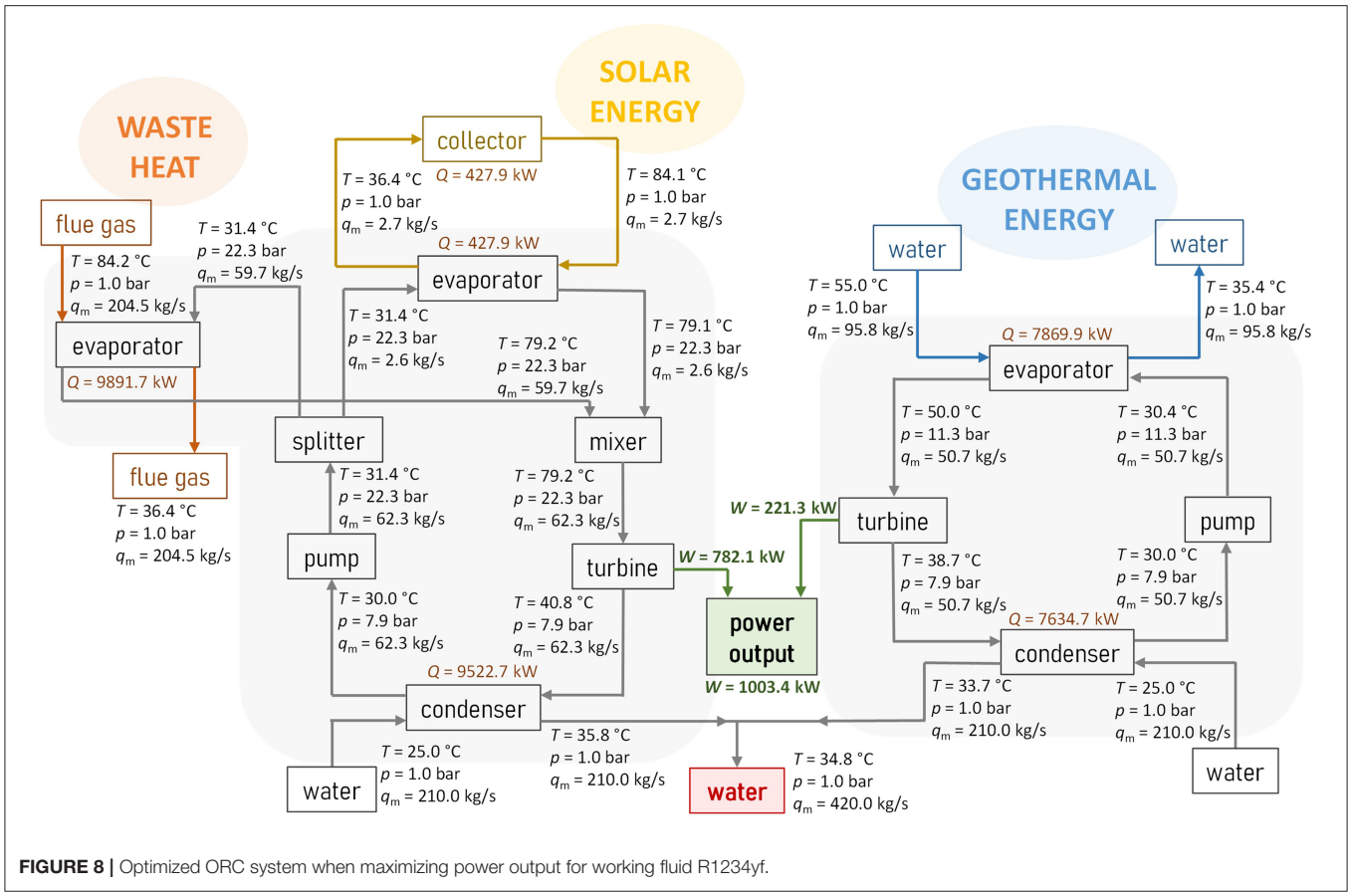

FIGURE 8 | Optimized ORC system when maximizing power output for working fluid R1234yf.

heat source and for all heat sources combined for the three working fluids considered. As it was presented above and shown in **Figure 1**, waste heat and solar energy are heat sources for one ORC cycle, while geothermal energy uses a separate ORC cycle.

Among used heat sources waste heat contributes the biggest proportion of generated electricity, especially in case of R245fa as a working fluid (830.4 kW). Other working fluids generate slightly less power output, R1234yf generates 782.1 kW and R1234ze generates 771.8 kW of power output.

Geothermal water has around half lower flowrate compared to flue gas (95.8 vs. 204.5 kg/s; see also **Figures 7–9**), but much lower electricity production due to lower temperature of geothermal energy (55 vs. 84.2°C). From **Figure 6** it could be also seen that solar energy contributes the least due to low annual average value of solar irradiance (see also **Figures 4**, **5**).

Figures 7–9 show optimized operating conditions of ORC system when maximizing power output for each working fluid, R245fa (**Figure 7**), R1234yf (**Figure 8**) and R1234ze (**Figure 9**). From Figures it can be seen that ORC loop (ORC-1) utilizing waste heat and solar energy provides comparably significantly higher power output compared to ORC loop utilizing geothermal energy (ORC-2). ORC-1 provides between 782.1 and 866.1 kW of power output, while ORC-2 provides between 221.3 and 246.5 kW of power output. The power output obtained from multiple heat source system is between 1003.4 and 1112.6 kW. For all the heat sources, the best results in terms of power output are achieved for working fluid R245fa, while the lowest power output is obtained for working fluid R1234yf.

In terms of operating conditions, similar values are obtained for all ORC systems using different working fluids. It can be seen that minimum approach temperature of 5°C occurred across all heat exchangers (evaporators and condensers). Flue gas is cooled down from 84.2° to 35–36°C, the fluid in solar collector circuit is heated up from around 35–36°C to around 80–84.2°C, while geothermal water is cooled down from 55°C to around 35°C. The highest flow is achieved for flue gas (204.5 kg/s), about half of that for geothermal water (95.8 kg/s), and significantly smaller for fluid in solar circuit (2.7–3.1 kg/s). On the other hand, the flowrate of produced hot water from the system is at the maximum level (set upper bound) of 210 kg/s for each ORC loop. The temperature of produced hot water is increased from 24°C to around 34.8°C in all three cases.

Regarding the ORC loops, the lowest flowrates are achieved for the optimized ORC system using working fluid R245fa (see **Figure 7**). In ORC-1 the flowrate is 47.7 kg/s, split mostly to waste heat evaporator (45.7 kg/s) and significantly less to solar heat evaporator (2 kg/s), while in ORC-2 the flowrate is 39.3 kg/s. Also, the pressures are the lowest in the ORC system utilizing R245fa as a working fluid (1.8/7.7 bar in ORC-1 and 1.8/3 bar in ORC-2). The other two working fluids operate at

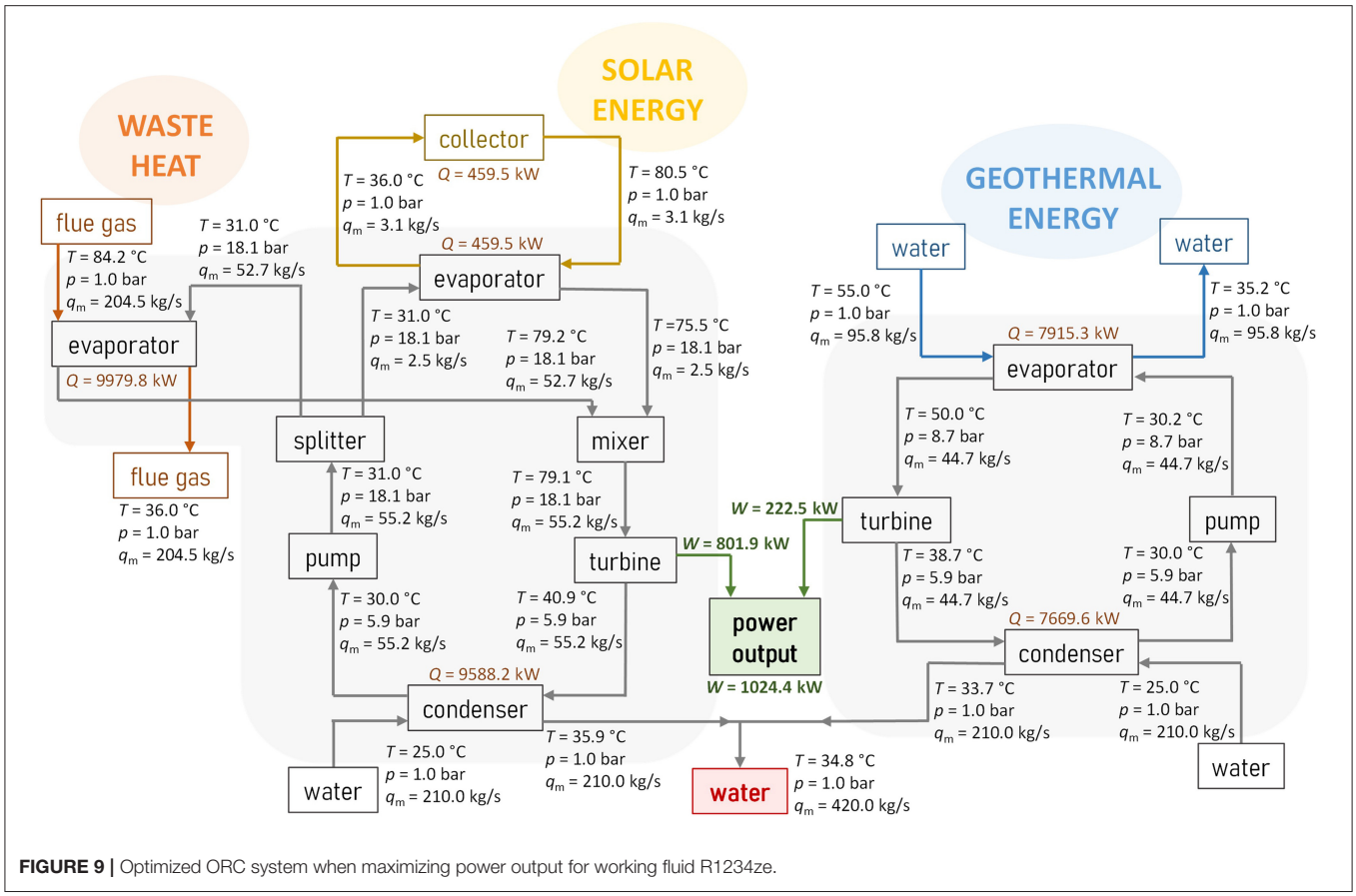

FIGURE 9 | Optimized ORC system when maximizing power output for working fluid R1234ze.

higher pressures, working fluid R1234yf operates at 7.9/22.3 bar in ORC-1 and 7.9/11.3 bar in ORC-2 (as shown in **Figure 8**) and working fluid R1234ze operates at 5.9/18.1 bar in ORC-1 and 5.9/8.7 bar in ORC-2 (as shown in **Figure 9**), which is according to liquid vapor pressure for used working fluids (see **Figure 2**).

The obtained results of power output for 12 monthly periods considering monthly average values of solar irradiance and ambient temperature are presented in **Figure 10**, which shows the electricity production of ORC-1 using waste heat and solar energy. It can be observed that ORC-1 produces power by utilized solar energy from March to September for all working fluids, while the contribution of utilized waste heat to the total electricity generation is constant throughout the year. The best performance of the system is achieved for all working fluids in June, with the highest power output obtained with the working fluid R245fa (979.7 kW) compared to the other two fluids R1234yf (886.2 kW) and R1234ze (913.3 kW). However, the contribution of utilized solar energy is relatively small compared to the power generation from waste heat, accounting for about 3% of the total electricity production from ORC-1 in March and about 15% in June. By adding the share of power generated from geothermal energy, the entire system has the highest electricity yield of 1226.3 kW in June.

When comparing the results of different time grids for ORC with R245fa, it should be noted that the optimal values indicate a difference of 35.8 kW (in January) and 113.6 kW (in June) in the maximum power output of the ORC-1 turbine for annual and monthly averages. The design of the system is tailored according to the optimal operating conditions, since many of them are assumed to be design or sizing variables. For example, the turbine design assumed for the annual average data will be oversized in the winter months, while the turbine capacity will not provide the maximum amount of electricity production in the summer months. Similar considerations apply to other equipment, particularly the characteristics of piping, pumps, and heat exchangers.

Maximizing Revenue From Heat and Electricity Production

The second objective considered in the study is maximization of the revenue of the system obtained from selling the power and heat produced in the ORC system. For the second objective, similar results are obtained as when maximizing power output. **Table 2** shows the main results for all three working fluids when maximizing the revenue of the system. As it can be seen the power output is the same as in **Figures 7–9**, and also the same values of variables are obtained for the optimized ORC systems. In terms

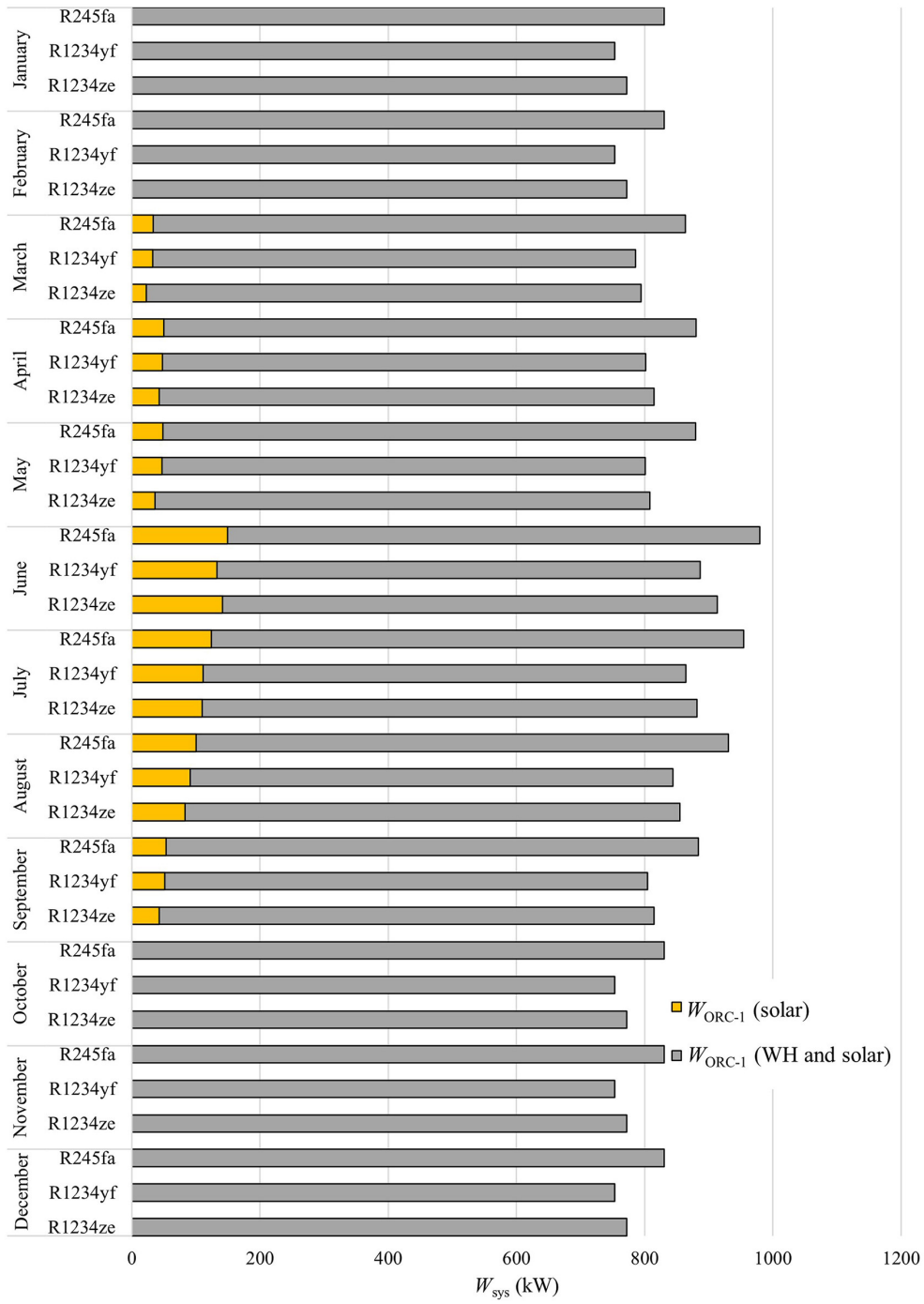

FIGURE 10 | Power output of ORC-1 obtained from waste heat and solar in monthly periods.

of revenue, significantly higher revenue is obtained from selling the heat compared to that for electricity, see also **Figure 11**.

Despite assumed significantly higher value of electricity price (0.08 €/kWh) compared to heat price (0.0243 €/kWh), revenue from selling heat is higher due to much larger energy contained in hot water compared to power output from the turbines. In terms of energy content, electricity share is only around 5–6%, while thermal energy share around 94–95%. As shown in **Figure 11**, the contribution of ORC-1 (waste heat and solar energy) to the share of revenue from selling heat is around 77–79%, while the share of revenue from electricity amounts to around 21–23%. ORC-2 contributes more to the share of revenue due to selling heat (91%), and much less to revenue due to selling electricity (9%).

TABLE 2 | Main results obtained by maximizing the revenue from ORC system.

	R245fa		R1234yf		R1234ze	
	ORC-1	ORC-2	ORC-1	ORC-2	ORC-1	ORC-2
$R_{heat,sys}$(10^6€/y)	2.04	1.64	2.03	1.63	2.04	1.63
$R_{elec,sys}$(10^6€/y)	0.61	0.17	0.55	0.16	0.56	0.16
W_{sys} (kW)	866.11	246.51	782.14	221.26	801.89	222.54
C_{TCI}(10^6€)	7.33	1.58	7.27	1.59	7.29	1.60
C_{OC}(10^6€/y)	1.94	0.83	1.97	0.84	1.96	0.84
R_{sys}(10^6€/y)	4.45		4.36		4.39	
NPV (10^6€)	7.68		6.46		6.72	
t_{PB} (y)	7.07		7.47		7.38	

The economic analysis (see **Table 2**) shows that total capital expenditure (C_{TCI}) for ORC-1 is around $7.3{\cdot}10^6$ €, while for ORC-2 C_{TCI} is about 4–5 times lower and is only around $1.6{\cdot}10^6$ €. On the other hand, operating cost are only about 2.3 times lower for ORC-2 compared to ORC-1. In case of all the working fluids, positive net present value (*NPV*) is obtained and is between 6.5 and $7.7{\cdot}10^6$ €, the highest for the fluid R245fa. Payback time (t_{PB}) in all three cases is between 7 and 7.5 y.

To investigate the impact of the discount rate on the economic performance of the system, a sensitivity analysis was further performed. The change in economic parameters such as *NPV* and t_{PB} within the studied discount rate interval of 2–14% is illustrated in **Figure 12**. The obtained results show similar trends for all working fluids, among which ORC with R245fa has the best performance, as the *NPV* is higher and t_{PB} is lower compared to ORC with the other two fluids (R1234yf and R1234ze). The increase in *p* leads to a decrease in *NPV* and increase in t_{PB}, which shows the dominance of capital cost over operating cost. It can be concluded that low discount rates have a positive impact on the economic performance of the system, since higher values of *NPV* and lower payback periods are obtained.

Limitations of the Work

The results of optimization presented in this paper are based on a case study that considers the use of multiple heat sources. In a Slovenian city, low-temperature waste heat in the form of flue gas from an aluminum smelter and low-temperature geothermal energy together with solar energy are available for utilization. It should be noted that the proposed design of ORC is tailored to the characteristics of a heat source, in particular its temperature, which reflects a certain inflexibility in terms of application of heat sources with different temperature ranges. For the evaluation of economic performance, mostly fixed values of economic parameters are assumed except for the discount rate, which lacks the information about the performance of the system in relation to the variability of these parameters. Furthermore, for realistic ORC design it is important to capture fluctuations on both the supply and demand sides, and thus multiperiod approach should be applied. However, while multi-period optimization presents improvements over single-period optimization, there are computational limitations which enable only a certain (usually low) number of periods that can be considered (Demirhan et al., 2020). To adequately solve such multiperiod problems that include shorter time periods, various solution strategies, application of clustering methods and employment of efficient solution algorithms is required. Another issue to be considered in the use of solar energy is the option of storage, which is not taken into account in this study. Notwithstanding certain simplifying assumptions that may be relaxed in future work, this study sheds light on the thermodynamic feasibility and economic viability of such a system.

CONCLUSIONS

In this study, an integrated design of hybrid ORC system is investigated that combines three heat sources, waste heat from aluminum smelter's flue gas, solar and geothermal energy, which provides insight into the development of renewable and sustainable energy systems and shows the good applicability of ORC using multiple heat sources. Due to two different temperature levels of heat sources (80–85 and 55°C) two separate ORC cycles are considered as this was beneficial for improved efficiency of the system. Maximum thermodynamic and economic performances were studied by considering objectives of maximizing power output and maximizing revenue from heat and electricity produced in ORC system.

The obtained results show that up to 830.4 kW of power could be produced from waste heat (see also Dokl et al., 2021), up to 246.5 kW from geothermal energy and up to 35.9 kW from solar energy. However, it should be noted that according to the low average value of solar radiation such small power output may not reflect the real situation. When all the heat sources are utilized, the system could produce up to 1112.6 kW of power. The highest values were obtained for all the heat sources when working fluid R245fa is used, while other two fluids provide slightly lower power outputs. Minimal power output is obtained for the fluid R1234yf and was about 90% of the power produced using fluid R245fa. Considering monthly periods, electricity generation is the highest in June obtained by working fluid R245fa (1226.3 kW), where 979.7 kW is generated from solar energy and waste heat, while geothermal energy contributed 246.5 kW.

Economic performance show that significantly more revenue is obtained while selling heat compared to the revenue obtained

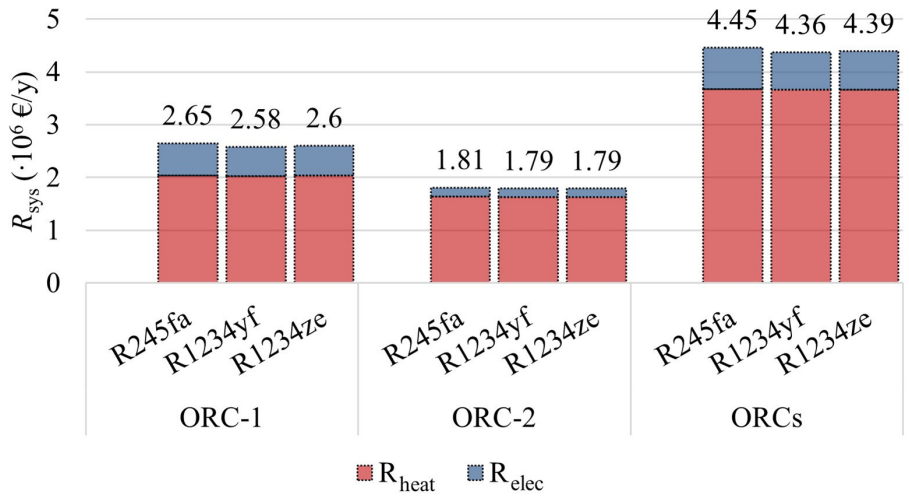

FIGURE 11 | Maximum values of revenue for optimized ORC system.

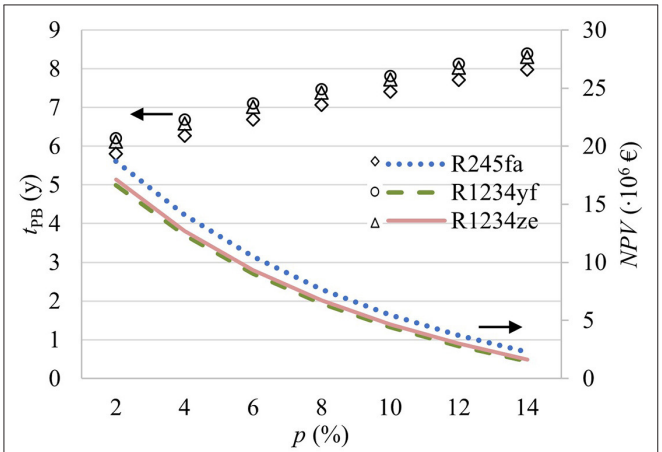

FIGURE 12 | Payback period and net present value vs. discount rate.

while selling electricity. Around 83% of revenue is obtained from selling heat while 17% from selling electricity. However, in terms of energy content, electricity contributes to only around 5–6%, while thermal energy to around 94–95%. The integrated system exhibits greater revenues than the cost and thus positive net present value for all considered discount rates (2–14%) and 20 years lifetime of the system. Sensitivity analysis regarding the influence of the discount rate on the economic performance of the system also showed the positive impact of lower discount rates, as higher NPV values and lower payback periods were obtained.

Future work will focus on a robust multiperiod approach to consider the fluctuating nature of renewable energy sources, especially of intermittent sources such as solar energy. Multi-period NLP model considering hourly, daily, and monthly time periods will thus be developed. Further, other medium and high temperature heat sources will be taken into account, such as biomass and waste, and the combination of ORC and heat pump technologies will be studied to explore the synergy among technologies enhancing energy efficiency. Finally, other heat recovery technologies for power production (such as Kalina, steam Rankine cycle), different architectures [cascade configuration, advanced cycle architectures and cycle modifications (Lecompte et al., 2015)], different solar thermal collector types [collectors for low and medium temperatures (Akhter et al., 2021)], different temperatures of flue gas and geothermal energy, and other design features will be explored to optimize the performance of energy conversion systems.

DATA AVAILABILITY STATEMENT

The original contributions presented in the study are included in the article/supplementary material, further inquiries can be directed to the corresponding author/s.

AUTHOR CONTRIBUTIONS

MD and LČ conducted the modeling and optimization of the proposed design and prepared the original draft. LČ and ZK reviewed and edited the manuscript. All authors contributed to the conceptual model design, to the article and approved the submitted version.

FUNDING

The authors are grateful for funding support from the Slovenian Research Agency (research core fundings No. P2-0412, P2-0421 and P2-0414 and projects No. N2-0138 and J7-3149).

REFERENCES

Abikoye, B., Čuček, L., Isafiade, A. J., and Kravanja, Z. (2019). Integrated design for direct and indirect solar thermal utilization in low temperature industrial operations. *Energy* 182, 381–396. doi: 10.1016/j.energy.2019.05.205

Abikoye, B., Čuček, L., Urbancl, D., Isafiade, A. J., and Kravanja, Z. (2020). Synthesis of heat pump enhanced solar thermal for low and medium temperature operations. *Comput. Aided Chem. Eng.* 48, 979–984. doi: 10.1016/B978-0-12-823377-1.50164-6

Akhter, J., Gilani, S. I., Al-Kayiem, H. H., Mehmood, M., Ali, M., Ullah, B., et al. (2021). Experimental investigation of a medium temperature single-phase thermosyphon in an evacuated tube receiver coupled with compound parabolic concentrator. *Front. Energy Res.* 9, 754546. doi: 10.3389/fenrg.2021.754546

Anastasovski, A., Rasković, P., and Guzović, Z. (2020). A review of heat integration approaches for organic rankine cycle with waste heat in production processes. *Energy Conversion Manag.* 221, 113175. doi: 10.1016/j.enconman.2020.113175

Andreasen, J. G., Baldasso, E., Kærn, M. R., Weith, T., Heberle, F., Brüggemann, D., et al. (2021). Techno-economic feasibility analysis of zeotropic mixtures and pure fluids for organic Rankine cycle systems. *Appl. Therm. Eng.* 192, 116791. doi: 10.1016/j.applthermaleng.2021.116791

Angelino, L., Kiruja, J., Bertelsen, N., Mathiesen, B. V., Djørup, S. R., Schneider, N. C. A., et al. (2021). *Integrating Low-Temperature Renewables in District Energy Systems*: *Guidelines for Policy Makers*.

Anvari, S., Khalilarya, S., and Zare, V. (2019). Power generation enhancement in a biomass-based combined cycle using solar energy: thermodynamic and environmental analysis. *Appl. Therm. Eng.* 153, 128–141. doi: 10.1016/j.applthermaleng.2019.02.112

Aspen Technology (2022). *Aspen Plus, The Chemical Industry's Leading Process Simulation Software* [Online]. Available online at: <*aspentech.com/en/products/engineering/aspen-plus*> (accessed January 29, 2022).

Bellos, E., and Tzivanidis, C. (2018). Investigation of a hybrid ORC driven by waste heat and solar energy. *Energy Conversion Manag.* 156, 427–439. doi: 10.1016/j.enconman.2017.11.058

Brough, D., and Jouhara, H. (2020). The aluminium industry: a review on state-of-the-art technologies, environmental impacts and possibilities for waste heat recovery. *Int. J. Thermofluids* 1–2:100007. doi: 10.1016/j.ijft.2019.100007

Castelli, A. F., Elsido, C., Scaccabarozzi, R., Nord, L. O., and Martelli, E. (2019). Optimization of organic rankine cycles for waste heat recovery from aluminum production plants. *Front. Energy Res.* 7, 44. doi: 10.3389/fenrg.2019.00044

Chen, H., Goswami, D. Y., and Stefanakos, E. K. (2010). A review of thermodynamic cycles and working fluids for the conversion of low-grade heat. *Renewable Sustain. Energy Rev.* 14, 3059–3067. doi: 10.1016/j.rser.2010.07.006

Christodoulides, P., Agathokleous, R., Aresti, L., Kalogirou, S. A., Tassou, S. A., and Florides, G. A. (2022). Waste heat recovery technologies revisited with emphasis on new solutions, including heat pipes, and case studies. *Energies* 15, 384. doi: 10.3390/en15010384

Demirhan, C. D., Boukouvala, F., Kim, K., Song, H., Tso, W. W., Floudas, C. A., et al. (2020). An integrated data-driven modeling and global optimization approach for multi-period nonlinear production planning problems. *Comput. Chem. Eng.* 141, 107007. doi: 10.1016/j.compchemeng.2020.107007

Dokl, M., Čuček, L., Abikoye, B., and Kravanja, Z. (2021). Maximizing the power output and net present value of Organic Rankine Cycle: application to aluminium industry. *Energy* 239, 122620. doi: 10.1016/j.energy.2021.122620

Egieya, J. M., Čuček, L., Zirngast, K., Isafiade, A. J., and Kravanja, Z. (2020). Optimization of biogas supply networks considering multiple objectives and auction trading prices of electricity. *BMC Chem. Eng.* 2, 3. doi: 10.1186/s42480-019-0025-5

Epp, B., and Oropeza, M. (2017). *Solar Heat for Industry* [Online]. Solar Payback. Available online at: <solar-payback.com/wp-content/uploads/2017/07/Solar-Heat-for-Industry-Solar-Payback-April-2017.pdf> (accessed January 31, 2022).

Gomaa, M. R., Mustafa, R. J., Al-Dhaifallah, M., and Rezk, H. (2020). A low-grade heat Organic Rankine Cycle driven by hybrid solar collectors and a waste heat recovery system. *Energy Rep.* 6, 3425–3445. doi: 10.1016/j.egyr.2020.12.011

Haghighi, A., Pakatchian, M. R., Assad, M. E. H., Duy, V. N., and Alhuyi Nazari, M. (2021). A review on geothermal Organic Rankine cycles: modeling and optimization. *J. Therm. Anal. Calorim.* 144, 1799–1814. doi: 10.1007/s10973-020-10357-y

Isafiade, A. J., Kravanja, Z., and Bogataj, M. (2016). Design of integrated solar thermal energy system for multi-period process heat demand. *Chem. Eng. Trans.* 52, 1303–1308. doi: 10.3303/CET1652218

Jahangir, M. H., Mousavi, S. A., and Vaziri Rad, M. A. (2019). A techno-economic comparison of a photovoltaic/thermal organic Rankine cycle with several renewable hybrid systems for a residential area in Rayen, Iran. *Energy Conversion Manag.* 195, 244–261. doi: 10.1016/j.enconman.2019.05.010

Kalikatzarakis, M., and Frangopoulos, C. (2015). Multi-criteria selection and thermo-economic optimization of Organic Rankine Cycle system for a marine application. *Int. J. Thermodyn.* 18, 133–141. doi: 10.5541/ijot.5000075305

Lam, H. L., Klemeš, J. J., and Kravanja, Z. (2011). Model-size reduction techniques for large-scale biomass production and supply networks. *Energy* 36, 4599–4608. doi: 10.1016/j.energy.2011.03.036

LEA Ptuj (2010). *Lokalni Energetski Koncept OBCINE KIDRICEVO*. Available online at: kidricevo.si/wp-content/uploads/2013/07/javno_lek_lek_kidricevo.pdf (accessed December 5, 2021).

Lecompte, S., Huisseune, H., van den Broek, M., Vanslambrouck, B., and De Paepe, M. (2015). Review of organic rankine cycle (ORC) architectures for waste heat recovery. *Rene. Sustain. Energy Rev.* 47, 448–461. doi: 10.1016/j.rser.2015.03.089

Lecompte, S., Oyewunmi, O. A., Markides, C. N., Lazova, M., Kaya, A., Van den Broek, M., et al. (2017). Case study of an Organic Rankine Cycle (ORC) for waste heat recovery from an Electric Arc Furnace (EAF). *Energies* 10, 649. doi: 10.3390/en10050649

Loni, R., Mahian, O., Markides, C. N., Bellos, E., le Roux, W. G., Kasaeian, A., et al. (2021a). A review of solar-driven Organic Rankine Cycles: recent challenges and future outlook. *Renewable Sustain. Energy Rev.* 150, 111410. doi: 10.1016/j.rser.2021.111410

Loni, R., Najafi, G., Bellos, E., Rajaee, F., Said, Z., and Mazlan, M. (2021b). A review of industrial waste heat recovery system for power generation with organic rankine cycle: recent challenges and future outlook. *J. Clean. Prod.* 287, 125070. doi: 10.1016/j.jclepro.2020.125070

Mahmoudi, A., Fazli, M., and Morad, M. R. (2018). A recent review of waste heat recovery by Organic Rankine Cycle. *Appl. Therm. Eng.* 143, 660–675. doi: 10.1016/j.applthermaleng.2018.07.136

Pang, K.-C., Chen, S.-C., Hung, T.-C., Feng, Y.-Q., Yang, S.-C., Wong, K.-W., et al. (2017). Experimental study on organic Rankine cycle utilizing R245fa, R123 and their mixtures to investigate the maximum power generation from low-grade heat. *Energy* 133, 636–651. doi: 10.1016/j.energy.2017.05.128

Papapetrou, M., Kosmadakis, G., Cipollina, A., La Commare, U., and Micale, G. (2018). Industrial waste heat: estimation of the technically available resource in the EU per industrial sector, temperature level and country. *Appl. Therm. Eng.* 138, 207–216. doi: 10.1016/j.applthermaleng.2018.04.043

Pierobon, L., Nguyen, T.-V., Larsen, U., Haglind, F., and Elmegaard, B. (2013). Multi-objective optimization of Organic Rankine Cycles for waste heat recovery: application in an offshore platform. *Energy* 58, 538–549. doi: 10.1016/j.energy.2013.05.039

Seider, W. D., Seader, J. D., Lewin, D. R., and Widagdo, S. (2009). *Product and Process Design Principles, Synthesis, Analysis, and Evaluation, Third Edition.* Hoboken, NJ, USA: John Wiley and Sons.

Senturk Acar, M., and Arslan, O. (2019). Energy and exergy analysis of solar energy-integrated, geothermal energy-powered Organic Rankine Cycle. *J. Therm. Anal. Calorim.* 137, 659–666. doi: 10.1007/s10973-018-7977-1

Sun, Q., Wang, Y., Cheng, Z., Wang, J., Zhao, P., and Dai, Y. (2020). Thermodynamic and economic optimization of a double-pressure organic Rankine cycle driven by low-temperature heat source. *Renewable Energy* 147, 2822–2832. doi: 10.1016/j.renene.2018.11.093

Toselli, D., Heberle, F., and Brüggemann, D. (2019). Techno-economic analysis of hybrid binary cycles with geothermal energy and biogas waste heat recovery. *Energies* 12, 1969. doi: 10.3390/en12101969

Wahlroos, M., Pärssinen, M., Rinne, S., Syri, S., and Manner, J. (2018). Future views on waste heat utilization – Case of data centers in Northern Europe. *Renew. Sustain. Energy Rev.* 82, 1749–1764. doi: 10.1016/j.rser.2017.10.058

Walraven, D., Laenen, B., and D'haeseleer, W. (2015). Economic system optimization of air-cooled organic Rankine cycles powered by low-temperature geothermal heat sources. *Energy* 80, 104–113. doi: 10.1016/j.energy.2014.11.048

Yang, J., Gao, L., Ye, Z., Hwang, Y., and Chen, J. (2021). Binary-objective optimization of latest low-GWP alternatives to R245fa for Organic Rankine Cycle application. *Energy* 217, 119336. doi: 10.1016/j.energy.2020.119336

Zhang, H., Guan, X., Ding, Y., and Liu, C. (2018). Emergy analysis of Organic Rankine Cycle (ORC) for waste heat power generation. *J. Clean. Prod.* 183, 1207–1215. doi: 10.1016/j.jclepro.2018.02.170

Zhang, W., Maleki, A., Birjandi, A. K., Alhuyi Nazari, M., and Mohammadi, O. (2020). Discrete optimization algorithm for optimal design of a solar/wind/battery hybrid energy conversion scheme. *Int. J. Low Carbon Technol.* 16, 326–340. doi: 10.1093/ijlct/ctaa067

Zore, Ž., Čuček, L., Širovnik, D., Novak Pintarič, Z., and Kravanja, Z. (2018). Maximizing the sustainability net present value of renewable energy supply networks. *Chem. Eng. Res. Des.* 131, 245–265. doi: 10.1016/j.cherd.2018.01.035

Conflict of Interest: The authors declare that the research was conducted in the absence of any commercial or financial relationships that could be construed as a potential conflict of interest

The handling editor AI declared a past co-authorship with the authors LČ, ZK.

Publisher's Note: All claims expressed in this article are solely those of the authors and do not necessarily represent those of their affiliated organizations, or those of the publisher, the editors and the reviewers. Any product that may be evaluated in this article, or claim that may be made by its manufacturer, is not guaranteed or endorsed by the publisher.

NOMENCLATURE

Sets

DPO	Set of maximal number of days in a month (31 days) with elements $dpo \in DPO$
DPOD	Set of pairs of original daily period *dpo* and merged daily period *dp*, $(dpo, dp) \in DPOD$
DPM	Set of pairs of original durations which regularizes the number of days in a month since the months contains different number of days $mp \in MP$, $dp \in DP$, $hp \in HP$, $(dp, mp) \in DPM$
HPO	Set of all hours in the day (24 hours) with elements $hpo \in HPO$
HPOH	Set of pairs of original hourly period *hpo* and merged hourly periods *hp*, $(hpo, hp) \in HPOH$
IO	Set of inlet and outlet streams with elements $io \in IO$; *K*, Set of time periods (year) with elements $k \in K$
MPO	Set of all months in the year with elements $mpo \in MPO$
MPOM	Set of pairs of original monthly period *mpo* and merged monthly periods *mp*, $(mpo, mp) \in MPOM$
U	Set of process units with elements $u \in U$

Subsets

COLL(*u*)	Collector as a process unit with element $coll \in COLL$
COND (*u*)	Condenser as a process unit with element $cond \in COND$
DP (*DPO*)	Set of discretised or merged monthly time period with elements $dp \in DP$
EVAP (*u*)	Evaporator as a process unit with element $evap \in EVAP$
HP (*HPO*)	Set of discretised or merged hourly time period with elements $hp \in HP$
IN (*IO*)	Inlet streams to process units with elements $in \in IN$
MIX (*u*)	Mixer as a process unit with element $mix \in MIX$
MP (*MPO*)	Set of discretised or merged monthly time period with elements $mp \in MP$
OUT (*IO*)	Outlet streams from process units with elements $out \in OUT$
PUMP (*u*)	Pump as a process unit with element $pump \in PUMP$
SPLIT (*u*)	Splitter as a process unit with element $split \in SPLIT$
TURB (*u*)	Turbine as a process unit with element $turb \in TURB$

Parameters

a_1, a_2	Experimental constants for thermal loss coefficient of solar collector (kW/(m^2 · °C))
A_{coll}	Area of collector (m^2)
c_{elec}	Price of electricity (€/kWh)
c_{heat}	Price of heat (€/kWh)
$Cn, n \in \{1, 2, ..., 13\}$	Coefficients for correlation
$T_{amb,mp,dp,hp}$, $T'_{amb,mp,dp,hp}$	Average solar irradiation and hourly solar irradiation for each hour of the year (W/m^2)
$T_{amb,mp,dp,hp}$, $T'_{amb,mp,dp,hp}$	Average ambient temperature and ambient temperature for each hour of the year (°C)
t_{OH}	Number of operating hours (h/y)
η_{turb}	Mechanical efficiency of turbine
ΔT_{min}	Minimum approach temperature (°C)
Π_0	Efficiency factor for solar collection

Variables

C_{OC}	Operating cost (€/y)
C_{TCI}	Total capital investment (€)
$h_{u,io}$	Mass enthalpy in the stream (kJ/kg)
NPV	Net present value (€)
$p_{u,io}$	Pressure in the stream (bar)
q_m	Mass flowrate (kg/s)
Q_u	Heat duty (kW)
R_{elec}	Revenue from electricity production (€/y)
t_{PB}	Payback period (y)
$T_{u,io}$	Temperature in the stream (°C)
W_{sys}	Power delivered by system (kW)
W_u	Produced power (kW)
η_{irrev}	Irreversibility factor